Flocking for Multiple Elliptical Agents With Limited Communication Ranges

Khac Duc Do

Abstract—**In existing flocking and coordination control systems of multiple agents, an agent is considered as a single point or a circular disk. For agents with a long and narrow shape, fitting them to circular disks results in a problem with the large conservative area. This paper presents a design of distributed controllers for flocking of N mobile agents with an elliptical shape and with limited communication ranges. A separation condition for elliptical agents is first derived. Smooth or p-times differentiable step functions are then introduced. These functions and the separation condition between the elliptical agents are embedded in novel potential functions to design control algorithms for flocking. The controllers guarantee 1) no switchings in the controllers despite the agents' limited communication ranges; 2) no collisions between any agents; 3) asymptotic convergence of each agent's generalized velocity to a desired velocity; and 4) boundedness of the flock size, which is defined as the sum of all generalized distances between the agents, by a constant.**

Index Terms—**Collision avoidance, elliptical agents, flocking, potential functions.**

I. Introduction

FLOCKING is the collective motion of a large number of self-propelled entities. For several decades, flocking has attracted attention of researchers in biology, physics, and computer science [1]–[4]. Engineering applications of flocking include search, rescue, coverage, surveillance, sensor networks, and cooperative transportation [5]–[15].

Heuristically, Reynolds [2] introduced three rules of flocking: 1) separation: avoid collision with nearby flock mates; 2) alignment: attempt to match velocity with nearby flock mates; and 3) cohesion: attempt to stay close to nearby flock mates. Since then, a number of modifications and extensions of these three rules and additional rules have been proposed and resulted in many algorithms to realize these rules [15]–[22]. For example, graph theory [16], [18] and the Lyapunov direct method [19] were used to solve a consensus problem, local attractive/repulsive potential between neighboring agents to deal with separation and a cohesion problem [22], and artificial potentials [13], [15], [21], [23], [24] for obstacle avoidance. The leader–follower approach to a target-tracking problem was used in [25] and [20]. Other related works include geometric formation optimization [26], [27], pattern formation [28], and task allocation [29]. In all the aforecited references, the agents are considered as a single point with an exception for [9], [10], [30], where the agents have a circular shape.

Manuscript received October 13, 2010; revised February 11, 2011; accepted June 2, 2011. Date of publication July 5, 2011; date of current version October 6, 2011. This paper was recommended for publication by Associate Editor K. Kyriakopoulos and Editor G. Oriolo upon evaluation of the reviewers comments. This work was supported in part by the Australian Research Council under Grant DP0988424.

The author is with the School of Mechanical Engineering, The University of Western Australia, Crawley, W.A. 6009, Australia (e-mail: duc@mech.uwa.edu.au).

Color versions of one or more of the figures in this paper are available online at http://ieeexplore.ieee.org.

Digital Object Identifier 10.1109/TRO.2011.2159410

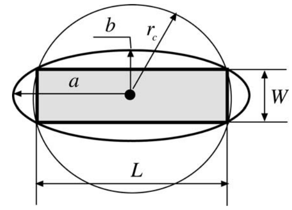

Fig. 1. Fitting a rectangular agent to an ellipse and a circle.

In practice, many agents such as surface ships have a noncircular, especially long and narrow, shape. If these agents are fitted to circular disks, there is a problem of the large conservative area. To illustrate this problem, we look at an example to fit a rectangular agent with a width of W and a length of L to an elliptical disk with semiaxes of a and b, and a circular disk with a radius of r_c as shown Fig. 1. By shrinking the space along the direction of the major axis of the ellipse that bounds the elliptical disk, we can find $a = \frac{\sqrt{2}}{2}W$, $b = \frac{\sqrt{2}}{2}L$, and $r_c = \frac{1}{2}\sqrt{W^2 + L^2}$. Therefore, the conservative area A_{con}, which is defined as the difference between the areas enclosed by the circle and the ellipse, is given by $A_{\mathrm{con}} = \pi r_c^2 - \pi ab = \frac{\pi}{4}(L - W)^2$. This means that the conservative area is proportional to the square of the difference between the width and the length of an agent.

A circular approximation of long and narrow agents' shape can adversely affect the performance of a flocking algorithm. An example is the case where it is necessary to flock a group of long and narrow agents through a long and narrow passageway. In some cases, a circular approximation of the agents's shape can result in failure of a flocking algorithm. As an illustration, we consider two agents with lengths of L_1 and L_2, and widths of W_1 and W_2. Assuming that W_1 and W_2 are much less than L_1 and L_2, respectively, i.e., the two agents have a long and narrow shape. We now require these two agents to flock in a way that the distance d_{12} between them is such that $\frac{W_1+W_2}{2} + \epsilon_{12} < d_{12} < \frac{L_1+L_2}{2} - \epsilon_{12}$ with ϵ_{12} being a feasible positive constant. A circular approximation of the agents' shape is not applicable in this case for a flocking algorithm. On the other hand, an elliptical approximation can be applicable. In addition, an elliptical approximation of the agents' shape for collision avoidance between the agents in a flocking algorithm covers a circular approximation of the agents' shape by setting the semiaxes of the bounding ellipse equal, but not vice versa.

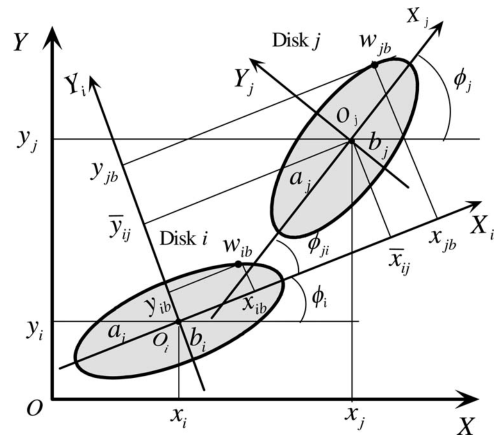

Fig. 2. Two elliptical disks and their coordinates.

The previous discussion indicates that it is much more efficient to use an elliptical approximation of the agents with a long and narrow shape for collision avoidance in designing flocking algorithms.

Despite the aforementioned advantages of an elliptical approximation of the agents' shape, flocking for elliptical agents has not been addressed in the literature. This is partially due to difficulties in determining a separation condition between two ellipses. For two elliptical disks, both the minimum distance between them [31] and the discriminant of their characteristic polynomial [32] methods are too complicated for an application in flock control. If these methods are applied for collision avoidance, the condition, for which the minimum distance between two disks or the discriminant of their characteristic polynomial is positive, is difficult to be embedded in a proper potential function to design a flocking algorithm.

The aforementioned observations motivate contributions of this paper on a design of flocking algorithms for mobile agents with an elliptical shape and limited communication ranges. The paper's contributions include: 1) a new condition for separation between two elliptical disks (see Section II-A); 2) a new pairwise potential function for two elliptical agents (see Section IV-A1); and 3) a derivation of flocking algorithms that are based on the pairwise potential functions (see Section IV).

II. Preliminaries

A. Separation Condition Between Two Elliptical Disks

This section presents a condition for separation of two elliptical disks that are applicable to collision avoidance in the flock control design later. As such, we consider two elliptical disks i and j that are shown in Fig. 2. In this figure, OXY is the earth-fixed frame, $O_iX_iY_i$ is the body-fixed frame that is attached to ellipse i, (x_i, y_i) denotes the position of the center O_i, and ϕ_i is the heading angle of the disk i. These notations are similar for the disk j. Moreover, (a_i, b_i) and (a_j, b_j) denote the semiaxes of the disks i and j, respectively.

Lemma 2.1: Consider two elliptical disks i and j, of which bounding ellipses have semiaxes of (a_i, b_i) and (a_j, b_j), are centered at (x_i, y_i) and (x_j, y_j), and have heading angles of ϕ_i and ϕ_j, respectively (see Fig. 2). Define the *generalized distance* Δ_{ij} between the elliptical disks i and j as

$$\Delta_{ij} = \sqrt{\frac{\|\boldsymbol{Q}_{ij}\bar{\boldsymbol{p}}_{ij}\|^2 + \|\boldsymbol{Q}_{ji}\bar{\boldsymbol{p}}_{ji}\|^2}{2}} \tag{1}$$

where $\bar{\boldsymbol{p}}_{ij} = [\bar{x}_{ij}\ \ \bar{y}_{ij}]^T$

$$\boldsymbol{Q}_{ij} = \begin{bmatrix} -\dfrac{\kappa_{ij}\cos(\alpha_{ij})}{a_i(\kappa_{ij}+\hat{a}_j^2)} & -\dfrac{\kappa_{ij}\sin(\alpha_{ij})}{b_i(\kappa_{ij}+\hat{a}_j^2)} \\ \dfrac{\kappa_{ij}\sin(\alpha_{ij})}{a_i(\kappa_{ij}+\hat{b}_j^2)} & -\dfrac{\kappa_{ij}\cos(\alpha_{ij})}{b_i(\kappa_{ij}+\hat{b}_j^2)} \end{bmatrix} \tag{2}$$

and κ_{ij} is the largest root (the right most root) of the following equation:

$$\left(\frac{\hat{a}_j\hat{x}_{ij}}{\kappa_{ij}+\hat{a}_j^2}\right)^2 + \left(\frac{\hat{b}_j\hat{y}_{ij}}{\kappa_{ij}+\hat{b}_j^2}\right)^2 - 1 = 0. \tag{3}$$

All the variables $\hat{a}_j, \hat{b}_j, \bar{x}_{ij}, \bar{y}_{ij}, \hat{x}_{ij}, \hat{y}_{ij}$, and α_{ij} are defined as follows:

$$\begin{aligned} \hat{a}_j &= \frac{1}{\sqrt{T_a}}, \quad \hat{b}_j = \frac{1}{\sqrt{T_b}} \\ \begin{bmatrix} \hat{x}_{ij} \\ \hat{y}_{ij} \end{bmatrix} &= \begin{bmatrix} -\dfrac{\cos(\alpha_{ij})}{a_i} & -\dfrac{\sin(\alpha_{ij})}{b_i} \\ \dfrac{\sin(\alpha_{ij})}{a_i} & -\dfrac{\cos(\alpha_{ij})}{b_i} \end{bmatrix} \bar{\boldsymbol{p}}_{ij} \\ \alpha_{ij} &= 2\arctan\left(\frac{2(T_{11}T_{12}+T_{21}T_{22})}{T_{11}^2+T_{21}^2+T_{12}^2+T_{22}^2}\right) \end{aligned} \tag{4}$$

with

$$\begin{aligned} T_a &= (T_{11}^2+T_{21}^2)\cos^2(\alpha_{ij}) + (T_{11}T_{12}+T_{21}T_{22}) \\ &\quad \times \sin(2\alpha_{ij}) + (T_{12}^2+T_{22}^2)\sin^2(\alpha_{ij}) \\ T_b &= (T_{11}^2+T_{21}^2)\sin^2(\alpha_{ij}) - (T_{11}T_{12}+T_{21}T_{22}) \\ &\quad \times \sin(2\alpha_{ij}) + (T_{12}^2+T_{22}^2)\cos^2(\alpha_{ij}) \\ T_{11} &= \frac{a_i}{a_j}\cos(\phi_{ij}), \quad T_{12} = -\frac{b_i}{a_j}\sin(\phi_{ij}) \\ T_{21} &= \frac{a_i}{b_j}\sin(\phi_{ij}), \quad T_{22} = \frac{b_i}{b_j}\cos(\phi_{ij}) \\ x_{ij} &= x_i - x_j, \quad y_{ij} = y_i - y_j, \quad \phi_{ij} = \phi_i - \phi_j \\ [\bar{x}_{ij},\ \bar{y}_{ij}]^T &= \boldsymbol{R}_i[x_{ij},\ y_{ij}]^T \end{aligned} \tag{5}$$

where $\boldsymbol{R}_i = -\boldsymbol{R}^{-1}(\phi_i)$ with $\boldsymbol{R}(\bullet)$ being the rotational matrix, i.e., $\boldsymbol{R}(\bullet) = \begin{bmatrix} \cos(\bullet) & -\sin(\bullet) \\ \sin(\bullet) & \cos(\bullet) \end{bmatrix}$. The matrix $\boldsymbol{Q}_{ji}$ and the vector $\bar{\boldsymbol{p}}_{ji}$ are defined accordingly. The two elliptical disks are externally separated, i.e., the disks are outside of each other and do not contact with each other as in Fig. 2, if

$$\Delta_{ij} > 1. \tag{6}$$

Proof: See Appendix A.

Remark 2.1: Δ_{ij} is a differentiable function of $\bar{\boldsymbol{p}}_{ij}$, $\bar{\boldsymbol{p}}_{ji}$, and ϕ_{ij}. Moreover $\Delta_{ij} = \Delta_{ji}$.

B. p-Times Differentiable Step Function

This section presents a construction of p-times differentiable or smooth step functions. These functions are to be embedded into a potential function to avoid discontinuities in the control law due to the agents' communication limited ranges.

Definition 2.1: A scalar function $h(x, a, b)$ is said to be a p-times differentiable step function if it possesses the following properties:

$$\begin{aligned} &1)\ h(x, a, b) = 0 \quad \forall -\infty < x \leq a \\ &2)\ h(x, a, b) = 1 \quad \forall\, b \leq x < \infty \\ &3)\ 0 < h(x, a, b) < 1 \quad \forall\, x \in (a, b) \\ &4)\ h(x, a, b) \ \text{ is } p\text{-times differentiable} \end{aligned} \tag{7}$$

where p is a positive integer, $x \in \mathbb{R}$, and a and b are constants such that $a < b$. Moreover, if the function $h(x, a, b)$ is infinite times differentiable with respect to x, then it is said to be a smooth step function.

Lemma 2.2: Let the scalar function $h(x, a, b)$ be defined as

$$h(x, a, b) = \frac{\int_a^x f(\tau - a) f(b - \tau) d\tau}{\int_a^b f(\tau - a) f(b - \tau) d\tau} \tag{8}$$

with a and b being constants such that $a < b$, and the function $f(y)$ being defined as

$$\begin{aligned} &f(y) = 0, \qquad \text{if } y \leq 0 \\ &f(y) = g(y), \qquad \text{if } y > 0 \end{aligned} \tag{9}$$

where the function $g(y)$ has the following properties:

$$\begin{aligned} &1)\ g(\tau - a) g(b - \tau) > 0 \qquad \forall \tau \in (a, b) \\ &1)\ g(y) \ \text{ is } p\text{-times differentiable} \\ &3)\ \lim_{y \to 0^+} \frac{\partial^k g(y)}{\partial y^k} = 0,\ k = 1, \ldots, p-1 \end{aligned} \tag{10}$$

with p being a positive integer. Then, the function $h(x, a, b)$ is a p-times differentiable step function. Moreover, if $g(y)$ in (9) is replaced by $g(y) = e^{-1/y}$, then $h(x, a, b)$ is a smooth step function.

Proof (See [30]): Examples of the function $g(y)$ are $g(y) = y^p$ and $g(y) = \arctan(y^p)$ for any positive integer p. It is trivial to check that these functions satisfy all properties that are listed in (10). All the bump functions that are used in [33] and [15] can be derived from Lemma 2.2 by picking a proper function $g(y)$.

C. Barbalat-Like Lemma

The following Barbalat-like lemma is to be used in the stability analysis of the closed-loop system.

Lemma 2.3: Assume that a nonnegative scalar differentiable function $f(t)$ satisfies the following conditions:

$$1)\ \left|\frac{d}{dt} f(t)\right| \leq k_1 f(t), \forall t \geq 0, \quad 2)\ \int_0^\infty f(t) dt \leq k_2 \tag{11}$$

where k_1 and k_2 are positive constants, then $\lim_{t \to \infty} f(t) = 0$.

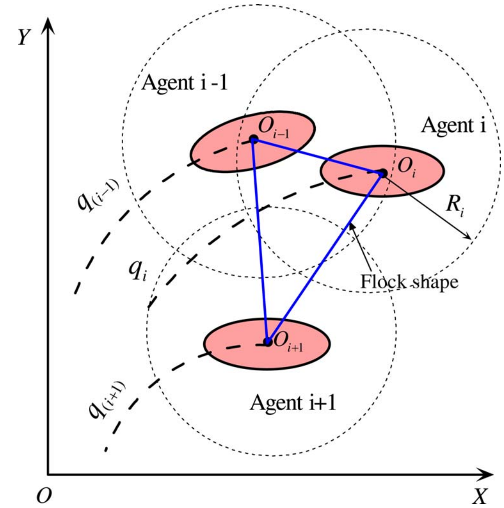

Fig. 3. Flocking setup.

Proof (See [8]): Lemma 2.3 differs from Barbalat's lemma that is found in [34]. While Barbalat's lemma assumes that $f(t)$ is uniformly continuous, Lemma 2.3 assumes that $|\frac{d}{dt} f(t)|$ is bounded by $k_1 f(t)$. Lemma 2.3 is useful in proving convergence of $f(t)$ when it is difficult to prove uniform continuity of $f(t)$.

III. Problem Statement

A. Agent Dynamics

As mentioned earlier, this paper mainly focuses on difficulties that are caused by the elliptical shape of the agents in the flocking control; we, therefore, assume that each elliptical agent i has the following dynamics:

$$\dot{\boldsymbol{q}}_i = \boldsymbol{u}_i, \quad i \in \mathbb{N} \tag{12}$$

where $\mathbb{N}$ is the set of all agents in the group, $\boldsymbol{u}_i = [u_{xi}\ u_{yi}\ u_{\phi i}]^T$ is the control input vector of the agent i, and it is recalled that $\boldsymbol{q}_i = [x_i\ y_i\ \phi_i]^T$ with (x_i, y_i) being the position of the center of the agent i, i.e., the center of the bounding ellipse i, and ϕ_i being the heading angle of the agent i (see Fig. 2). For agents with higher order dynamics, the backstepping technique [35] can be used because we will design the control $\boldsymbol{u}_i$ that is differentiable as many times as desired.

B. Flock Control Objective

In order to design a flocking algorithm for a group of elliptical agents, there is a need to specify a common goal for the group, some communication between the agents, and initial position and orientation of the agents. We, therefore, impose the following assumption on communication and initial conditions between the agents and the flocking rendezvous trajectory—a trajectory for all the agents in the group to track.

Assumption 3.1

1) The agents i and j have circular communication areas, which are centered at points O_i and O_j, and have radii of R_i and R_j (see Fig. 3). The radii R_i and R_j are sufficiently large

in the sense that

$$\Delta^m_{ijR} > 1 \tag{13}$$

where Δ^m_{ijR} is the greatest lower bound of Δ_{ij} when the agents i and j are within their communication ranges, i.e.,

$$\Delta^m_{ijR} = \inf(\Delta_{ij}) \text{ s.t. } \begin{cases} \phi_{ij} \in \mathbb{R} \\ \|\bar{\boldsymbol{p}}_{ij}\| = \min(R_i, R_j) \end{cases} \tag{14}$$

for all $(i, j) \in \mathbb{N}$ and $j \neq i$.

2) The agent i broadcasts its trajectory $\boldsymbol{q}_i$ in its communication area. Moreover, the agent i can receive the trajectory $\boldsymbol{q}_j$ that is broadcasted by other agents $j, j \in \mathbb{N}, j \neq i$ in the group if the points O_j of these agents are in the communication area of the agent i.

3) At the initial time $t_0 \geq 0$, all the agents in the group are sufficiently far away from each other in the sense that the following condition holds:

$$\Delta_{ij}(t_0) > 1 \tag{15}$$

where $\Delta_{ij}(t_0)$ is given in (1) evaluated at $\boldsymbol{q}_i = \boldsymbol{q}_i(t_0)$ and $\boldsymbol{q}_j = \boldsymbol{q}_j(t_0)$, and we have abused the notation of $\Delta_{ij}(\bar{\boldsymbol{p}}_{ij}(t_0), \bar{\boldsymbol{p}}_{ji}(t_0), \phi_{ij}(t_0))$ as $\Delta_{ij}(t_0)$ for simplicity of presentation.

4) The flocking rendezvous trajectory $\boldsymbol{q}_{od} = [x_{od}, y_{od}, \phi_{od}]^T$ for all the agents to track has a bounded derivative $\dot{\boldsymbol{q}}_{od}$ and is available to all the agents.

Remark 3.1

1) In item 1, Condition (13) holds if there exists a positive constant ϱ_i such that $R_i \geq \varrho_i + \max(a_i + a_j, b_i + b_j, a_i + b_j, a_j + b_i)$, for all $(i, j) \in \mathbb{N}$ and $j \neq i$.

2) Items 1 and 2 in Assumption 3.1 specify the way each agent communicates with other agents in the group within its communication range. In Fig. 3, the agents i and $i-1$ are communicating with each other since the points O_{i-1} and O_i are in the communication areas of the agents i and $i-1$, respectively. The agents i and $i+1$ are not communicating with each other since the points O_i and O_{i+1} are not in the communication areas of the agents $i+1$ and i, respectively. In other words, the agents in the group are connected if they are inside their communication ranges.

3) Item 3 in Assumption 3.1 implies from Lemma 2.1 that at the initial time t_0, there is no collision between any agents in the group.

4) Items 1–3 in Assumption 3.1 do not guarantee overall connectivity among all the agents in the group in general. Under item 4 in Assumption 3.1, we do not require overall connectivity among all the agents to design a flocking algorithm.

5) Item 4 in Assumption 3.1 means that all the agents are aware of the flocking rendezvous trajectory. This item together with items 1 and 2 in Assumption 3.1 were also required in [15] to design a nonfragmentation flocking algorithm for *point* agents based on an attractive/repulsive potential field. In [15], Olfati-Saber also showed that under items 1 and 2 if all the agents are not aware of the flocking rendezvous trajectory, the flocking algorithm works only for a very restricted set of initial states and a small number of agents. In [21], a further analysis of the flocking algorithm that is proposed in [15] was carried out for the case where only several agents in a group are aware of the flocking rendezvous trajectory. It was shown in [21] that the agents, which are not aware of the flocking rendezvous trajectory and stay disconnected from the other agents in the group sufficiently long, would stay disconnected from the agents, which are aware of the flocking rendezvous trajectory, i.e., the flocking algorithm leads to fragmentation. Hence, this paper imposes item 4 in Assumption 3.1 to design a flocking algorithm for elliptical agents. It is possible to use the analysis technique in [21] to analyze the flocking algorithm to be proposed later in this paper for elliptical agents when only several agents are aware of the flocking rendezvous trajectory. This is because the flocking algorithm that is to be designed in this paper is also based on an attractive/repulsive potential field. However, since this paper focuses on solving difficulties due to an elliptical shape of the agents for collision avoidance in a flocking algorithm, all the agents are assumed to be aware of the flocking rendezvous trajectory.

Flock Control Objective 3.1: Under Assumption 3.1, for each agent i design the control input vector $\boldsymbol{u}_i$ to achieve a desired flocking that include: 1) no switchings in the controllers; 2) no collisions between any agents; 3) asymptotic convergence of each agent's generalized velocity to a desired velocity; and 4) boundedness of the flock size $F_L(t) = \sum_{j=i+1}^{N} \sum_{j=1}^{i-1} \Delta_{ij}(t)$ by a constant when the time t tends to infinity.

IV. Flock Control Design

Under Assumption 3.1, several approaches that are mentioned in Section I can be used to design a flocking algorithm that achieves the flock control objective 3.1. Each approach has its own advantages and disadvantages. For example, the leader–follower approach can be used by 1) designing a virtual leader to be moved on the flocking rendezvous trajectory; 2) generating a virtual structure whose center is the virtual leader such that as the virtual structure moves, its vertices generate collision-free trajectories; and 3) designing a control law for each agent to track a collision-free trajectory traced out by a vertex of the virtual structure. As such, this approach would result in a simple control design. However, a collision among the agents might occur during the transient response. Moreover, this approach has a difficulty to deal with a change in the number of the agents because it requires to regenerate a virtual structure.

This section presents a method to design a flocking algorithm that achieves the flock control objective 3.1 using the potential function approach. Roughly speaking, the proposed control design is to force all the agents to track the flocking rendezvous trajectory and to separate the agents if they are sufficiently close to each other. Although all the agents need to know the flocking rendezvous trajectory that they are all trying to track, each agent does not need its own reference trajectory to track. Consequently, the flocking control design is scalable to the number of the agents. Moreover, smooth pairwise potential functions are constructed in Section IV-A1 to separate the agents locally, i.e., the repulsive field resulted from the pairwise potential functions is active only if the agents are sufficiently close to each other.

A. Potential Function

1) Pairwise Potential Function: This section defines and constructs pairwise potential functions that will be used in a Lyapunov function for the flock control design.

Definition 4.1: Let φ_{ij} be a scalar function of the generalized distance Δ_{ij} that is given in (1) of the elliptical agents i and j. The function φ_{ij} is said to be a pairwise potential function if it has the following properties:

$$\begin{aligned}
&1)\ \varphi_{ij}=k_{ij},\ \frac{\partial\varphi_{ij}}{\partial\Delta_{ij}}=0,\ \frac{\partial^2\varphi_{ij}}{\partial\Delta_{ij}^2}=0\quad\forall\,\Delta_{ij}\in[\Delta_{ijR}^M,\infty)\\
&2)\ \varphi_{ij}>0\quad\forall\,\Delta_{ij}\in(1,\Delta_{ijR}^M)\\
&3)\ \lim_{\Delta_{ij}\to1^+}\varphi_{ij}=\infty,\ \lim_{\Delta_{ij}\to1^+}\frac{\partial\varphi_{ij}}{\partial\Delta_{ij}}=-\infty\\
&4)\ \varphi_{ij}\ \text{is at least twice differentiable}\quad\forall\,\Delta_{ij}\in(1,\infty)\\
&5)\ \varphi_{ij}\ \text{has a unique minimum value at}\ \Delta_{ij}=\Delta_{ijd}\\
&\quad\forall\,\Delta_{ij}\in(1,\Delta_{ijR}^M)
\end{aligned}\tag{16}$$

where k_{ij} is a positive constant. The positive constant Δ_{ijd} is referred to as the desired generalized distance between the agents i and j and must satisfy the condition

$$1<\Delta_{ijd}<\Delta_{ijR}^m \tag{17}$$

with Δ_{ijR}^m being defined in (14). The constant Δ_{ijR}^M is the least upper bound of the generalized distance Δ_{ij} when the agents i and j are within their communication ranges, i.e.,

$$\Delta_{ijR}^M=\sup(\Delta_{ij})\quad\text{s.t.}\quad\begin{cases}\phi_{ij}\in\mathbb{R}\\ \|\bar{\boldsymbol{p}}_{ij}\|=\min(R_i,R_j).\end{cases}\tag{18}$$

Remark 4.1: Property 1 implies that the function φ_{ij} is constant when the agents i and j are outside of their communication ranges. Property 2 implies that the function φ_{ij} is positive definite when the agents i and j are inside of their communication ranges. By Lemma 2.1, Property 3 means that the function φ_{ij} is equal to infinity when a collision between the agents i and j occurs. Property 4 allows us to use control design and stability analysis methods that are found in [34] for continuous systems instead of techniques for switched and discontinuous systems that are found in [36] to handle the collision-avoidance problem under the agents' limited communication ranges. Property 5 makes it effective to use a gradient-based method for the flock control design.

Lemma 4.1: Let the scalar function φ_{ij} be defined as

$$\varphi_{ij}=\gamma_{ij}\frac{1-h(\chi_{ij},a_{ij},b_{ij})}{\chi_{ij}}+k_{ij}h(\chi_{ij},a_{ij},b_{ij})\tag{19}$$

$$\begin{aligned}
\gamma_{ij}&=\frac{1}{2}\left(\sqrt{\Delta_{ij}^2+\epsilon^2\Delta_{ijd}^2}-\sqrt{1+\epsilon^2}\Delta_{ijd}\right)^2\\
\chi_{ij}&=\frac{1}{2}\left(\sqrt{\Delta_{ij}^2+\epsilon^2}-\sqrt{1+\epsilon^2}\right)^2
\end{aligned}\tag{20}$$

with ϵ being a positive constant. The positive constants a_{ij} and b_{ij} satisfy the condition

$$a_{ij}=\chi_{ijd},\qquad a_{ij}<b_{ij}\le\chi_{ijR}^M\tag{21}$$

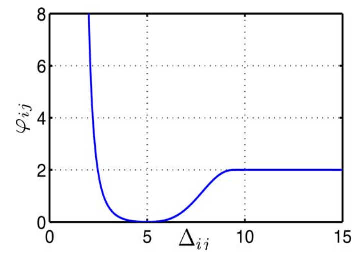

Fig. 4. Pairwise potential function.

where χ_{ijd} and χ_{ijR}^M are given by

$$\begin{aligned}
\chi_{ijR}^M&=\frac{1}{2}\left(\sqrt{\left(\Delta_{ijR}^M\right)^2+\epsilon^2}-\sqrt{1+\epsilon^2}\right)^2\\
\chi_{ijd}&=\frac{1}{2}\left(\sqrt{\Delta_{ijd}^2+\epsilon^2}-\sqrt{1+\epsilon^2}\right)^2.
\end{aligned}\tag{22}$$

The positive constant k_{ij} is chosen such that

$$\varphi_{ij}'>0\tag{23}$$

for all $\Delta_{ij}\in(\Delta_{ijd},\Delta_{ijR}^M)$ or equivalently $\chi_{ij}\in(\chi_{ijd},\chi_{ijR}^M)$, where $\varphi_{ij}'=\frac{\partial\varphi_{ij}}{\partial\chi_{ij}}$ and is given by

$$\begin{aligned}
\varphi_{ij}'&=\gamma_{ij}'\frac{1-h(\chi_{ij},a_{ij},b_{ij})}{\chi_{ij}}+k_{ij}h'(\chi_{ij},a_{ij},b_{ij})\\
&\quad-\gamma_{ij}\frac{h'(\chi_{ij},a_{ij},b_{ij})\chi_{ij}+(1-h(\chi_{ij},a_{ij},b_{ij}))}{\chi_{ij}^2}
\end{aligned}\tag{24}$$

with $\gamma_{ij}'=\frac{\partial\gamma_{ij}}{\partial\chi_{ij}}$. The function $h_{ij}\big(\chi_{ij},a_{ij},b_{ij}\big)$ is a p-times differentiable step function that is defined in Definition 2.1 with $p\ge2$ and $g(y)=y^p$.

Then, the function φ_{ij} is a pairwise potential function.

Proof (See Appendix B): A pairwise potential function φ_{ij} with $\epsilon=1,\Delta_{ijd}=5,\Delta_{ijR}^M=10,p=2,a_{ij}=\chi_{ijd}$, and $b_{ij}=0.9\chi_{ijR}^M$ is plotted in Fig. 4.

2) Potential Function: Having constructed the pairwise potential function φ_{ij} for the agents i and j, the potential function φ for all the agents in the group is the sum of all the pairwise potential functions, i.e.,

$$\varphi=\sum_{i=1}^{N-1}\sum_{j=i+1}^{N}\varphi_{ij}\tag{25}$$

where φ_{ij} is given in (19).

B. Derivative of Potential Function

To prepare for the flock control design later, we calculate the derivative of φ_{ij} by differentiating both sides of (25) to obtain

$$\dot\varphi=\sum_{i=1}^{N-1}\sum_{j=i+1}^{N}\frac{\partial\varphi_{ij}}{\partial(\Delta_{ij}^2)}\frac{d\Delta_{ij}^2}{dt}.\tag{26}$$

From (1), we have $\Delta_{ij}^2=\frac{1}{2}\big(\|\boldsymbol{Q}_{ij}\bar{\boldsymbol{p}}_{ij}\|^2+\|\boldsymbol{Q}_{ji}\bar{\boldsymbol{p}}_{ji}\|^2\big)$ and note from (2)–(5) that $\boldsymbol{Q}_{ij}$ depends on $\bar{\boldsymbol{p}}_{ij}$, κ_{ij}, and ϕ_{ij}. We first calculate the first time derivative of κ_{ij}. Let us define

$$F_{ij} = \left(\frac{\hat{a}_j \hat{x}_{ij}}{\kappa_{ij} + \hat{a}_j^2}\right)^2 + \left(\frac{\hat{b}_j \hat{y}_{ij}}{\kappa_{ij} + \hat{b}_j^2}\right)^2 \tag{27}$$

which is a smooth function of κ_{ij}, $\bar{\boldsymbol{p}}_{ij}$, and ϕ_{ij}. Differente both sides of (3) to obtain $\dot{\kappa}_{ij}$ as

$$\dot{\kappa}_{ij} = -\left(\frac{\partial F_{ij}}{\partial \kappa_{ij}}\right)^{-1}\left(\left(\frac{\partial F_{ij}}{\partial \bar{\boldsymbol{p}}_{ij}}\right)^T \dot{\bar{\boldsymbol{p}}}_{ij} + \frac{\partial F_{ij}}{\partial \phi_{ij}}\dot{\phi}_{ij}\right). \tag{28}$$

It is noted that $\frac{\partial F_{ij}}{\partial \kappa_{ij}}$ is always nonzero (see Appendix A-B). Hence, the first time derivative of Δ_{ij}^2 is

$$\frac{d\Delta_{ij}^2}{dt} = \boldsymbol{G}_{ij}\dot{\bar{\boldsymbol{p}}}_{ij} + \boldsymbol{G}_{ji}\dot{\bar{\boldsymbol{p}}}_{ji} + H_{ij}\dot{\phi}_{ij} + H_{ji}\dot{\phi}_{ji} \tag{29}$$

where

$$\begin{aligned}
\boldsymbol{G}_{ij} &= (\boldsymbol{Q}_{ij}\bar{\boldsymbol{p}}_{ij})^T\left(\boldsymbol{Q}_{ij} - \frac{1}{\frac{\partial F_{ij}}{\partial \kappa_{ij}}}\frac{\partial \boldsymbol{Q}_{ij}}{\partial \kappa_{ij}}\bar{\boldsymbol{p}}_{ij}\left(\frac{\partial F_{ij}}{\partial \bar{\boldsymbol{p}}_{ij}}\right)^T\right)\\
\boldsymbol{G}_{ji} &= (\boldsymbol{Q}_{ji}\boldsymbol{p}_{ji})^T\left(\boldsymbol{Q}_{ji} - \frac{1}{\frac{\partial F_{ji}}{\partial \kappa_{ji}}}\frac{\partial \boldsymbol{Q}_{ji}}{\partial \kappa_{ji}}\bar{\boldsymbol{p}}_{ji}\left(\frac{\partial F_{ji}}{\partial \bar{\boldsymbol{p}}_{ji}}\right)^T\right)\\
H_{ij} &= (\boldsymbol{Q}_{ij}\bar{\boldsymbol{p}}_{ij})^T\left(\frac{\partial \boldsymbol{Q}_{ij}}{\partial \phi_{ij}}\bar{\boldsymbol{p}}_{ij} - \frac{1}{\frac{\partial F_{ij}}{\partial \kappa_{ij}}}\frac{\partial \boldsymbol{Q}_{ij}}{\partial \kappa_{ij}}\bar{\boldsymbol{p}}_{ij}\frac{\partial F_{ij}}{\partial \phi_{ij}}\right)\\
H_{ji} &= (\boldsymbol{Q}_{ji}\bar{\boldsymbol{p}}_{ji})^T\left(\frac{\partial \boldsymbol{Q}_{ji}}{\partial \phi_{ji}}\bar{\boldsymbol{p}}_{ji} - \frac{1}{\frac{\partial F_{ji}}{\partial \kappa_{ji}}}\frac{\partial \boldsymbol{Q}_{ji}}{\partial \kappa_{ji}}\bar{\boldsymbol{p}}_{ji}\frac{\partial F_{ji}}{\partial \phi_{ji}}\right).
\end{aligned} \tag{30}$$

From the definitions of $\bar{\boldsymbol{p}}_{ij}$ and $\bar{\boldsymbol{p}}_{ji}$ in (2), we have

$$\dot{\bar{\boldsymbol{p}}}_{ij} = \boldsymbol{R}_i\left(\dot{\boldsymbol{p}}_{ij} + \boldsymbol{S}\boldsymbol{p}_{ij}\dot{\phi}_i\right) \tag{31}$$

where $\boldsymbol{R}_i = -\boldsymbol{R}^{-1}(\phi_i)$, $\boldsymbol{S} = \left[\begin{smallmatrix}0 & 1\\ -1 & 0\end{smallmatrix}\right]$, $\boldsymbol{p}_i = [x_i\ y_i]^T$, and $\boldsymbol{p}_{ij} = \boldsymbol{p}_i - \boldsymbol{p}_j$, for all $(i,j) \in \mathbb{N}, i \neq j$. Now noting $\boldsymbol{p}_{ij} = \boldsymbol{p}_i - \boldsymbol{p}_{od} - (\boldsymbol{p}_j - \boldsymbol{p}_{od})$ and $\dot{\boldsymbol{p}}_{ij} = \dot{\boldsymbol{p}}_i - \dot{\boldsymbol{p}}_{od} - (\dot{\boldsymbol{p}}_j - \dot{\boldsymbol{p}}_{od})$ with $\boldsymbol{p}_{od} = [x_{od},\ y_{od}]^T$, and adding and subtracting $\boldsymbol{R}_i\boldsymbol{S}(\boldsymbol{p}_j - \boldsymbol{p}_{od})\dot{\phi}_j$ to the right-hand side of (31) results in

$$\begin{aligned}
\dot{\bar{\boldsymbol{p}}}_{ij} = \boldsymbol{R}_i\Big(&\dot{\boldsymbol{p}}_i - \dot{\boldsymbol{p}}_{od} + \boldsymbol{S}(\boldsymbol{p}_i - \boldsymbol{p}_{od})\dot{\phi}_i - \big(\dot{\boldsymbol{p}}_j - \dot{\boldsymbol{p}}_{od}\\
&+ \boldsymbol{S}(\boldsymbol{p}_j - \boldsymbol{p}_{od})\dot{\phi}_j\big) - \boldsymbol{S}(\boldsymbol{p}_j - \boldsymbol{p}_{od})\dot{\phi}_{ij}\Big).
\end{aligned} \tag{32}$$

Similarly, we have

$$\begin{aligned}
\dot{\bar{\boldsymbol{p}}}_{ji} = \boldsymbol{R}_j\Big(&\dot{\boldsymbol{p}}_j - \dot{\boldsymbol{p}}_{od} + \boldsymbol{S}(\boldsymbol{p}_j - \boldsymbol{p}_{od})\dot{\phi}_j - \big(\dot{\boldsymbol{p}}_i - \dot{\boldsymbol{p}}_{od}\\
&+ \boldsymbol{S}(\boldsymbol{p}_i - \boldsymbol{p}_{od})\dot{\phi}_i\big) - \boldsymbol{S}(\boldsymbol{p}_i - \boldsymbol{p}_{od})\dot{\phi}_{ji}\Big).
\end{aligned} \tag{33}$$

The substitution of (32) and (33) into (29) and then into (26) with a note that $\phi_{ij} = -\phi_{ji} = \phi_i - \phi_j = \phi_i - \phi_{od} - (\phi_j - \phi_{od})$ gives

$$\begin{aligned}
\dot{\varphi} = \sum_{i=1}^{N}\Bigg[&\Bigg(\sum_{j=i+1}^{N}\boldsymbol{\Gamma}_{ij} + \sum_{j=1}^{i-1}\boldsymbol{\Lambda}_{ij}\Bigg)\big(\dot{\boldsymbol{p}}_i - \dot{\boldsymbol{p}}_{od}\\
&+ \boldsymbol{S}(\boldsymbol{p}_i - \boldsymbol{p}_{od})\dot{\phi}_i\big) + \Bigg(\sum_{j=i+1}^{N}\Xi_{ij} - \sum_{j=1}^{i-1}\Xi_{ji}\Bigg)(\dot{\phi}_i - \dot{\phi}_{od})\Bigg]
\end{aligned} \tag{34}$$

where

$$\begin{aligned}
\boldsymbol{\Gamma}_{ij} &= \frac{\partial \varphi_{ij}}{\partial(\Delta_{ij}^2)}\Big(\boldsymbol{G}_{ij}\boldsymbol{R}_i - \boldsymbol{G}_{ji}\boldsymbol{R}_j\Big)\\
\boldsymbol{\Lambda}_{ji} &= \frac{\partial \varphi_{ij}}{\partial(\Delta_{ij}^2)}\Big(\boldsymbol{G}_{ji}\boldsymbol{R}_j - \boldsymbol{G}_{ij}\boldsymbol{R}_i\Big)\\
\Xi_{ij} &= \frac{\partial \varphi_{ij}}{\partial(\Delta_{ij}^2)}\Big(\big(H_{ij} - \boldsymbol{G}_{ij}\boldsymbol{R}_i\boldsymbol{S}\boldsymbol{p}_j\big) - \big(H_{ji} - \boldsymbol{G}_{ji}\boldsymbol{R}_j\boldsymbol{S}\boldsymbol{p}_i\big)\Big).
\end{aligned} \tag{35}$$

C. Lyapunov Function

We now construct a Lyapunov function candidate as a sum of the potential function φ in (25) and the square of errors $\boldsymbol{p}_i - \boldsymbol{p}_{od}$ and $\phi_i - \phi_{od}$ for the flock control design in the next section as follows:

$$V = \varphi + \frac{1}{2}\sum_{i=1}^{N}\Big(c_1\|\boldsymbol{R}_i(\boldsymbol{p}_i - \boldsymbol{p}_{od})\|^2 + c_2(\phi_i - \phi_{od})^2\Big) \tag{36}$$

where c_1 and c_2 are positive constants, and we used the error $\boldsymbol{R}_i(\boldsymbol{p}_i - \boldsymbol{p}_{od})$ instead of $(\boldsymbol{p}_i - \boldsymbol{p}_{od})$ to make the control design later possible due to the term $\big(\dot{\boldsymbol{p}}_i - \dot{\boldsymbol{p}}_{od} + \boldsymbol{S}(\boldsymbol{p}_i - \boldsymbol{p}_{od})\dot{\phi}_i\big)$ in (34). The differentiation of both sides of (36) along the solutions of (34) and recalling from (12) that $\dot{\boldsymbol{p}}_i = [u_{xi},\ u_{yi}]^T$ and $\dot{\phi}_i = u_{\phi i}$ results in

$$\begin{aligned}
\dot{V} = \sum_{i=1}^{N}\Bigg[&\Big[\Omega_{xi}\ \Omega_{yi}\Big]\left(\begin{bmatrix}u_{xi}\\ u_{yi}\end{bmatrix} - \dot{\boldsymbol{p}}_{od} + \boldsymbol{S}(\boldsymbol{p}_i - \boldsymbol{p}_{od})u_{\phi i}\right)\\
&+ \Omega_{\phi i}(u_{\phi i} - \dot{\phi}_{od})\Bigg]
\end{aligned} \tag{37}$$

where

$$\begin{aligned}
\begin{bmatrix}\Omega_{xi}\\ \Omega_{yi}\end{bmatrix} &= \sum_{j=i+1}^{N}\boldsymbol{\Gamma}_{ij}^T + \sum_{j=1}^{i-1}\boldsymbol{\Lambda}_{ij}^T + c_1(\boldsymbol{p}_i - \boldsymbol{p}_{od})\\
\Omega_{\phi i} &= \sum_{j=i+1}^{N}\Xi_{ij} - \sum_{j=1}^{i-1}\Xi_{ji} + c_2(\phi_i - \phi_{od}).
\end{aligned} \tag{38}$$

D. Control Law

From (37), to avoid a large control effort when an agent in the group is close to the agent i due to Property 3 of the function φ_{ij} (see (16), for collision avoidance), we design a control law for u_{xi}, u_{yi}, and $u_{\phi i}$ as follows:

$$\begin{aligned} u_{xi} &= -k_1\psi(\Omega_{xi}) + \dot{x}_{od} - (y_i - y_{od})u_{\phi i} \\ u_{yi} &= -k_2\psi(\Omega_{yi}) + \dot{y}_{od} + (x_i - x_{od})u_{\phi i} \\ u_{\phi i} &= -k_3\psi(\Omega_{\phi i}) + \dot{\phi}_{od} \end{aligned} \tag{39}$$

where k_1, k_2, and k_3 are positive constants. The function $\psi(x)$ is a scalar, differentiable, and bounded function, and satisfies

1) $|\psi(x)| \leq M_1$
2) $\psi(x) = 0 \quad \text{if } x = 0, \quad x\psi(x) > 0 \quad \text{if } x \neq 0$
3) $\psi(-x) = -\psi(x), (x - y)[\psi(x) - \psi(y)] \geq 0$
4) $\left|\frac{\psi(x)}{x}\right| \leq M_2, \quad \left|\frac{\partial\psi(x)}{\partial x}\right| \leq M_3, \quad \frac{\partial\psi(x)}{\partial x}\Big|_{x=0} = 1$ (40)

for all $x \in \mathbb{R}, y \in \mathbb{R}$, where M_1, M_2, and M_3 are the positive constants. Some functions that satisfy the aforementioned properties are $\arctan(x)$ and $\tanh(x)$. The substitution of the control law in (39) into (37) gives

$$\dot{V} = -\sum_{i=1}^{N}\omega_i \tag{41}$$

where

$$\begin{aligned} \omega_i &= k_1\Omega_{xi}\psi(\Omega_{xi}) + k_2\Omega_{yi}\psi(\Omega_{yi}) \\ &\quad + k_3\Omega_{\phi i}\psi(\Omega_{\phi i}). \end{aligned} \tag{42}$$

On the other hand, the substitution of the control law in (39) into (12) results in the closed-loop system

$$\begin{aligned} \dot{x}_i &= -k_1\psi(\Omega_{xi}) + \dot{x}_{od} - (y_i - y_{od})\big(-k_3\psi(\Omega_{\phi i}) + \dot{\phi}_{od}\big) \\ \dot{y}_i &= -k_2\psi(\Omega_{yi}) + \dot{y}_{od} + (x_i - x_{od})\big(-k_3\psi(\Omega_{\phi i}) + \dot{\phi}_{od}\big) \\ \dot{\phi}_i &= -k_3\psi(\Omega_{\phi i}) + \dot{\phi}_{od}. \end{aligned} \tag{43}$$

for all $i \in \mathbb{N}$. We now present the main result of our paper in the following theorem.

Theorem 4.1: Under Assumption 3.1, the differentiable control input, i.e., $\boldsymbol{u}_i = [u_{xi} \ \ u_{yi} \ \ , u_{\phi i}]^T$, whose components are given in (39) for the agent i solves the flocking control objective. In particular, the following results hold.

1) There are no collisions between any agents, and the closed-loop system (43) is forward complete.
2) The relative distance between each agent i and the flocking rendezvous trajectory $\boldsymbol{q}_{od}$ is bounded, i.e., $\|\boldsymbol{q}_i(t) - \boldsymbol{q}_{od}(t)\| \leq A_0$ for all $t \geq t_0 \geq 0$ with A_0 a constant that depends on the initial conditions.
3) The generalized velocity of each agent i asymptotically approaches the generalized flocking rendezvous velocity, i.e.,

$$\begin{aligned} &\lim_{t\to\infty}\big(\dot{x}_i(t) - \dot{x}_{od}(t) + (y_i(t) - y_{od}(t))\dot{\phi}_{od}(t)\big) = 0 \\ &\lim_{t\to\infty}\big(\dot{y}_i(t) - \dot{y}_{od}(t) - (x_i(t) - x_{od}(t))\dot{\phi}_{od}(t)\big) = 0 \\ &\lim_{t\to\infty}\big(\dot{\phi}_i(t) - \dot{\phi}_{od}(t)\big) = 0. \end{aligned} \tag{44}$$

4) The flock size $F_L(t) = \sum_{j=i+1}^{N}\sum_{j=1}^{i-1}\Delta_{ij}(t)$ is bounded by a positive constant as time tends to infinity, i.e.,

$$\lim_{t\to\infty} F_L(t) = F_{Lc} \tag{45}$$

with $F_{Lc} \leq c_0$, where c_0 is a positive constant.

Proof: See Appendix C.

V. Simulation Results

In this section, we provide a numerical simulation to illustrate the effectiveness of the proposed flocking control design that is stated in Theorem 4.1. We use $N = 25$ elliptical agents with the geometric parameters as $a_i = 6$ and $b_i = 2$ for all $i = 1, \ldots, N$. The initial position and orientation of these agents are chosen as follows. The agents $1, \ldots, 5$ and $6, \ldots, N$ are uniformly located on circles that are centered at $(10, 0)$ with radii of 18 and 40, respectively, and their headings are randomly chosen between 0 and 2π. Specifically

$$\boldsymbol{q}_i(0) = \begin{bmatrix} -R_0\cos\left(\frac{2\pi(i-1)}{N_0}\right) + 10 \\ -R_0\sin\left(\frac{2\pi(i-1)}{N_0}\right) \\ 2\pi\,\text{rand}(\bullet) \end{bmatrix} \tag{46}$$

where $R_0 = 18$ and $N_0 = 5$ for $i = 1, \ldots, 5$; $R_0 = 40$ and $N_0 = 20$ for $i = 6, \ldots, 15$; and rand($\bullet$) is a random number between 0 and 1. All the agents have the same communication range of $R_i = 20$. The control design parameters are chosen as follows: $k_1 = 10$, $k_2 = 10$, $k_3 = 5$, $c_1 = 0.5$, $c_2 = 0.5$, $k_{ij} = 2.5$, $\epsilon = 1$, $\Delta_{ijd} = 1.2$, $a_{ij} = \chi_{ijd}$, and $b_{ij} = 2a_{ij}$ for all $(i, j) \in \mathbb{N}, j \neq i$. The function $\psi(\cdot)$ is chosen as $\arctan(\cdot)$. The generalized flocking rendezvous trajectory and its velocity are generated by a unicycle mobile robot, i.e., $\dot{\boldsymbol{q}}_{od} = [u_{od}\cos(\phi_{od}),\, u_{od}\sin(\phi_{od}),\, r_{od}]^T$, where $u_{od} = 15$, $r_{od} = 15/R_d$ with $R_d = 40$. The initial condition is $\boldsymbol{q}_{od}(0) = [R_d,\, 0,\, \pi/2]^T$. This choice implies that the generalized flocking rendezvous trajectory is a circle that is centered at the origin and with a radius of R_d. A calculation shows that the initial conditions (46) and the aforementioned choice of control design parameters satisfy all the conditions (13), (15), (17), (21), (23). Simulation results are plotted in Figs. 5 and 6. The little dark color circular disk indicates the head of the agent. In Fig. 5, several snapshots of the position and orientation of all agents are plotted. The representative $\chi_{ij}^* = \left(\Pi_{j\in\mathbb{N}j\neq i}\chi_{ij}\right)^{1/21}$ is plotted in the first subfigure of Fig. 6. The control inputs $u_x = [u_{x1}, \ldots, u_{xi}, \ldots, u_{xN}]^T$, $u_y = [u_{y1}, \ldots, u_{yi}, \ldots, u_{yN}]^T$, and $u_\phi = [u_{\phi 1}, \ldots, u_{\phi i}, \ldots, u_{\phi N}]^T$ are plotted in the second, third, and fourth subfigures of Fig. 6. It is seen from Figs. 5 and 6 that there is no collision between any agents as indicated by $\chi_{ij}^* > 0$ for all $i \in \mathbb{N}$. Moreover, all the agents manage to track the generalized flocking rendezvous trajectory $\boldsymbol{q}_{od}$. The mismatched velocity can be seen from the second, third, and fourth subfigure of Fig. 6. The rotational velocity $u_{\phi i}$, i.e., $\dot{\phi}_i$, asymptotically converges to $\dot{\phi}_{od}$ (see the fourth subfigure of Fig. 6). The linear velocities u_{xi} and u_{yi}, i.e., $\dot{x}_i$ and $\dot{y}_i$, asymptotically converge to $(\dot{x}_{od} - (y_i - y_{od})\dot{\phi}_{od})$ and $(\dot{y}_{od} + (x_i - x_{od})\dot{\phi}_{od})$ as proven in Theorem 4.1.

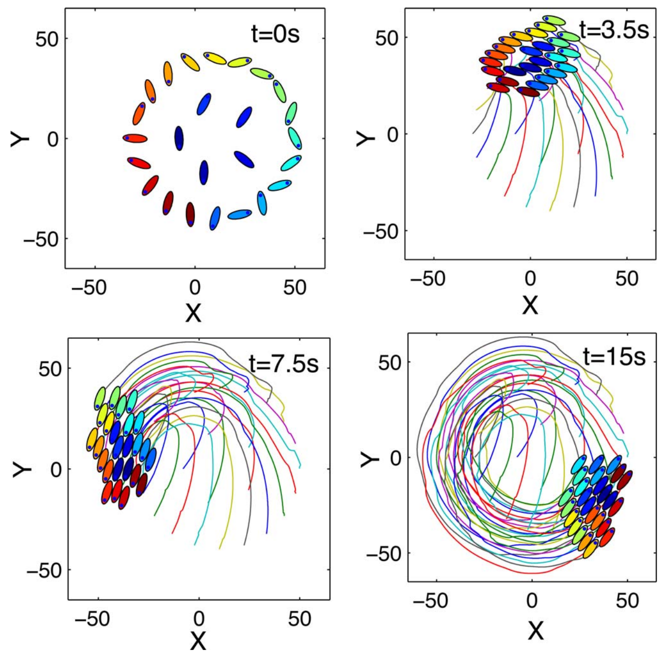

Fig. 5. Snapshots of the agents' position and orientation.

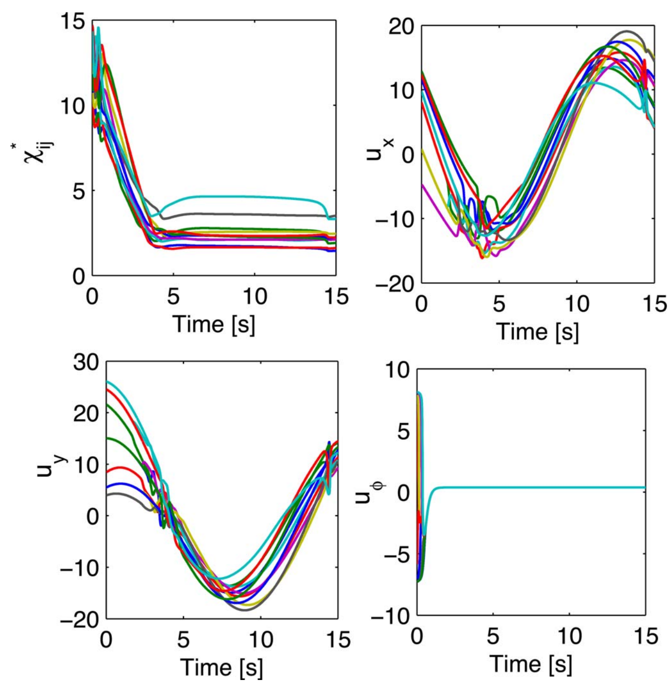

Fig. 6. Representative χ^*_{ij} and control inputs.

VI. Conclusion

A constructive method has been presented to design algorithms for flocking of N mobile agents with an elliptical shape and limited communication ranges. The flock control design is based on a separation condition for elliptical agents, smooth or p-times differentiable step functions, and Lyapunov's method through an introduction of novel potential functions. The proposed flock algorithms achieved desired flocking behaviors that include no switchings in the controllers despite agents' limited communication ranges, no collisions between any agents, asymptotic convergence of each agent's generalized velocity to a desired velocity, and boundedness of the flock size by a constant. An extension of the proposed flock control design and those controllers that are designed for single underactuated ships in [37] to provide a flock control system for multiple underactuated ships is under consideration.

Appendix A
Proof of Lemma 2.1

From Fig. 2, the boundaries of the disks i and j (equations of a point w_{ib} and w_{jb}) that are coordinated in the frame $O_iX_iY_i$ attached to the disk i can be described by

$$\mathrm{E}_i : \frac{x_{ib}^2}{a_i^2} + \frac{y_{ib}^2}{b_i^2} = 1$$

$$\mathrm{E}_j : \begin{bmatrix} x_{jb} \\ y_{jb} \end{bmatrix} = \begin{bmatrix} \bar{x}_{ij} \\ \bar{y}_{ij} \end{bmatrix} + \boldsymbol{R}^{-1}(\phi_{ij}) \begin{bmatrix} a_j \cos(\theta_j) \\ b_j \sin(\theta_j) \end{bmatrix} \tag{47}$$

where $\bar{x}_{ij}$, $\bar{y}_{ij}$, and ϕ_{ij} are defined in (5), and $\theta_j \in [0, 2\pi]$ is an auxiliary angle. The idea to prove Lemma 2.1 is first to transform the ellipses i and j to a circle and an ellipse. We then calculate the distance from the circle center to the transformed ellipse. As such, we propose the following coordinate transformation:

$$\begin{bmatrix} \hat{x}_{ib} \\ \hat{y}_{ib} \end{bmatrix} = \boldsymbol{R}^{-1}(\alpha_{ij}) \begin{bmatrix} \dfrac{x_{ib} - \bar{x}_{ij}}{a_i} \\ \dfrac{y_{ib} - \bar{y}_{ij}}{b_i} \end{bmatrix}$$

$$\begin{bmatrix} \hat{x}_{jb} \\ \hat{y}_{jb} \end{bmatrix} = \boldsymbol{R}^{-1}(\alpha_{ij}) \begin{bmatrix} \dfrac{x_{jb} - \bar{x}_{ij}}{a_i} \\ \dfrac{y_{jb} - \bar{y}_{ij}}{b_i} \end{bmatrix} \tag{48}$$

where α_{ij} is given in (4). With the coordinate changes (48), the ellipses i and j are transformed to

$$\mathrm{E}_i : (\hat{x}_{ib} - \hat{x}_{ij})^2 + (\hat{x}_{ib} - \hat{y}_{ij})^2 = 1$$

$$\mathrm{E}_j : \frac{\hat{x}_{jb}^2}{\hat{a}_j^2} + \frac{\hat{y}_{jb}^2}{\hat{b}_j^2} = 1 \tag{49}$$

where $\hat{x}_{ij}$ and $\hat{y}_{ij}$ are given in (4). Now, the ellipse i has become a unit circle that is centered at $(\hat{x}_{ij}, \hat{y}_{ij})$, while the ellipse j has become an ellipse that is centered at the origin and with semiaxes being $\hat{a}_j$ and $\hat{b}_j$ that is given in (4).

A. Distance Δ_{ij}

We now calculate the distance from the center of the unit circle that is described by the first equation in (49), i.e., from the point $(\hat{x}_{ij}, \hat{y}_{ij})$ to the ellipse that is described by the second equation in (49). The closest point $(\hat{x}_{jb}, \hat{y}_{jb})$ on the ellipse to the point $(\hat{x}_{ij}, \hat{y}_{ij})$ must occur so that $(\hat{x}_{ij} - \hat{x}_{jb}, \hat{y}_{ij} - \hat{y}_{jb})$ is normal to the ellipse. The orthogonality condition is

$$(\hat{x}_{ij} - \hat{x}_{jb}, \hat{y}_{ij} - \hat{y}_{jb}) = \kappa_{ij} \left(\frac{\hat{x}_{jb}}{\hat{a}_j^2}, \frac{\hat{y}_{jb}}{\hat{b}_j^2} \right) \tag{50}$$

where κ_{ij} is the largest root of the second equation in (49) and (50), i.e., (3). We must take κ_{ij} as the largest root of (3) so as to have the closest point $(\hat{x}_{jb}, \hat{y}_{jb})$ on the ellipse to the point $(\hat{x}_{ij}, \hat{y}_{ij})$. Because of symmetry, we only need to consider $\hat{x}_{ij} \geq 0$ and $\hat{y}_{ij} \geq 0$. From (50), we have

$$\hat{x}_{jb} = \frac{\hat{a}_j^2 \hat{x}_{ij}}{\kappa_{ij} + \hat{a}_j^2}, \quad \hat{y}_{jb} = \frac{\hat{b}_j^2 \hat{y}_{ij}}{\kappa_{ij} + \hat{b}_j^2}. \tag{51}$$

Since $\hat{x}_{jb} \geq 0$ and $\hat{y}_{jb} \geq 0$ with a note that $\hat{x}_{ij}$ and $\hat{y}_{ij}$ are not equal to zero simultaneously, we require $\kappa_{ij} > -\min(\hat{a}_j^2, \hat{b}_j^2)$. The substitution of (51) into the second equation in (49) results in (3). It is noted that the closest point $(\hat{x}_{jb}, \hat{y}_{jb})$ on the ellipse E_j in (49) such that $(\hat{x}_{ij} - \hat{x}_{jb}, \hat{y}_{ij} - \hat{y}_{jb})$ normal to the ellipse E_j in (49) corresponds to the largest root κ_{ij} of (3).

Now, the distance from the point $(\hat{x}_{ij}, \hat{y}_{ij})$ to the closest point $(\hat{x}_{jb}, \hat{y}_{jb})$ on the ellipse that is described by the second equation in (49) is given by

$$d_{ij} = \sqrt{\|\boldsymbol{Q}_{ij}\bar{\boldsymbol{p}}_{ij}\|^2} - 1 \tag{52}$$

where $\boldsymbol{Q}_{ij}$ and $\bar{\boldsymbol{p}}_{ij}$ are given in (4). Similarly, we transform the two ellipses j and i to a circle and an ellipse. The distance from the point $(\hat{x}_{ji}, \hat{y}_{ji})$, which is the center of the circle that is transformed from the ellipse j, to the closest point $(\hat{x}_{ib}, \hat{y}_{ib})$ on the ellipse (which is transformed from the ellipse i) is

$$d_{ji} = \sqrt{\|\boldsymbol{Q}_{ji}\bar{\boldsymbol{p}}_{ji}\|^2} - 1. \tag{53}$$

Therefore, two ellipses i and j are separated if both $d_{ij} > 0$ and $d_{ji} > 0$, i.e., condition (6) must hold. The reason why we use the distance Δ_{ij} in (1) instead of $\Delta_{ij} = d_{ij} + 1$ or $\Delta_{ij} = d_{ji} + 1$ is to create a symmetrical Δ_{ij} (see Remark 2.1). This is crucial for the success of our flocking design.

We now show that Δ_{ij} is differentiable with respect to $\bar{\boldsymbol{p}}_{ij}$, $\bar{\boldsymbol{p}}_{ji}$, and ϕ_{ij}. From the expression of Δ_{ij} in (1) and the matrix $\boldsymbol{Q}_{ij}$ in (2), it is readily shown that differentiability of κ_{ij} with respect to $\bar{\boldsymbol{p}}_{ij}$ and ϕ_{ij} implies that of Δ_{ij} with respect to $\bar{\boldsymbol{p}}_{ij}$, $\bar{\boldsymbol{p}}_{ji}$, and ϕ_{ij}. To show that κ_{ij} is differentiable with respect to $\bar{\boldsymbol{p}}_{ij}$ and ϕ_{ij}, we first find the domain on which (3) has the largest root. As such, from (3), we define

$$F(\bullet) = \left(\frac{\hat{a}_j \hat{x}_{ij}}{\kappa_{ij} + \hat{a}_j^2}\right)^2 + \left(\frac{\hat{b}_j \hat{y}_{ij}}{\kappa_{ij} + \hat{b}_j^2}\right)^2 - 1. \tag{54}$$

We calculate $\frac{\partial F(\bullet)}{\partial \kappa_{ij}}$ and $\frac{\partial^2 F(\bullet)}{\partial \kappa_{ij}^2}$ as follows:

$$\begin{aligned} \frac{\partial F(\bullet)}{\partial \kappa_{ij}} &= -2\left[\frac{(\hat{a}_j \hat{x}_{ij})^2}{(\kappa_{ij} + \hat{a}_j^2)^3} + \frac{(\hat{b}_j \hat{y}_{ij})^2}{(\kappa_{ij} + \hat{b}_j^2)^3}\right] \\ \frac{\partial^2 F(\bullet)}{\partial \kappa_{ij}^2} &= 6\left[\frac{(\hat{a}_j \hat{x}_{ij})^2}{(\kappa_{ij} + \hat{a}_j^2)^4} + \frac{(\hat{b}_j \hat{y}_{ij})^2}{(\kappa_{ij} + \hat{b}_j^2)^4}\right]. \end{aligned} \tag{55}$$

Observing that for any point $(\hat{x}_{ij}, \hat{y}_{ij})$ with $\hat{x}_{ij} \geq 0$ and $\hat{y}_{ij} \geq 0$ but $\hat{x}_{ij}$ and $\hat{y}_{ij}$ are not equal to zero simultaneously, we have from (55) that $\frac{\partial F(\bullet)}{\partial \kappa_{ij}} < 0$ and $\frac{\partial^2 F(\bullet)}{\partial \kappa_{ij}^2} > 0$ for $\kappa_{ij} \in (-\min(\hat{a}_j^2, \hat{b}_j^2), \infty)$. Moreover, since $\lim_{\kappa_{ij} \to -\min(\hat{a}_j^2, \hat{b}_j^2)^+} F(\bullet) = \infty$ and $\lim_{\kappa_{ij} \to \infty} F(\bullet) = -1$, the function $F(\bullet)$ is a strictly decreasing function for $\kappa_{ij} \in (-\min(\hat{a}_j^2, \hat{b}_j^2), \infty)$. Hence, (3) has a unique root on the domain $(-\min(\hat{a}_j^2, \hat{b}_j^2), \infty)$. This root is also the largest root of (3).

We now show that κ_{ij} is differentiable with respect to $\bar{\boldsymbol{p}}_{ij}$ and ϕ_{ij}. Since $F(\bullet) = 0$ and $\hat{x}_{ij}$ and $\hat{y}_{ij}$ are differentiable functions of $\bar{\boldsymbol{p}}_{ij}$ and ϕ_{ij} that are defined in (4), the differentiation of $F(\bullet) = 0$ with respect to $\bar{\boldsymbol{p}}_{ij}$ and ϕ_{ij}, respectively, results in

$$\begin{aligned} \frac{\partial \kappa_{ij}}{\partial \bar{\boldsymbol{p}}_{ij}} &= -\left(\frac{\partial F(\bullet)}{\partial \kappa_{ij}}\right)^{-1} \frac{\partial F(\bullet)}{\partial \bar{\boldsymbol{p}}_{ij}} \\ \frac{\partial \kappa_{ij}}{\partial \phi_{ij}} &= -\left(\frac{\partial F(\bullet)}{\partial \kappa_{ij}}\right)^{-1} \frac{\partial F(\bullet)}{\partial \phi_{ij}}. \end{aligned} \tag{56}$$

Since κ_{ij} needs to satisfy $\kappa_{ij} \in (-\min(\hat{a}_j^2, \hat{b}_j^2), \infty)$ as shown previously, we have from (55) that $\frac{\partial F(\bullet)}{\partial \kappa_{ij}} < 0$ for all $\kappa_{ij} \in (-\min(\hat{a}_j^2, \hat{b}_j^2), \infty)$. This plus differentiability of $F(\bullet)$ with respect to $\bar{\boldsymbol{p}}_{ij}$ and ϕ_{ij} implies from (56) that κ_{ij} is differentiable with respect to $\bar{\boldsymbol{p}}_{ij}$ and ϕ_{ij}.

B. *Solution of (3)*

Equation (3) can be written as a quartic equation in κ_{ij}. The quartic equation can be solved by using Ferrari's method [38], but it is extremely complicated (there are four roots, and it is not clear which root is the largest one.

Therefore, we here provide a procedure to solve (3) for κ_{ij} numerically. The convexity of $F(\kappa_{ij})$ on its domain, namely that $\frac{\partial^2 F(\kappa_{ij})}{\partial \kappa_{ij}^2} > 0$ for all $\kappa_{ij} \in (-\min(\hat{a}_j^2, \hat{b}_j^2), \infty)$), makes Newton's method [39] an ideal numerical method to locate the root for our case.

Given an initial guess $\kappa_{ij}(0)$, the Newton iterates are

$$\kappa_{ij}(n+1) = \kappa_{ij}(n) - \frac{F(\kappa_{ij}(n))}{\frac{\partial F(\kappa_{ij})}{\partial \kappa_{ij}}\Big|_{\kappa_{ij} = \kappa_{ij}(n)}}. \tag{57}$$

It is important to choose an initial guess for which the method converges. Newton's method has an intuitive geometric appeal to it. The next value $\kappa_{ij}(n+1)$ is computed by determining where the tangent line to the graph at $(\kappa_{ij}(n), F(\kappa_{ij}(n)))$ intersects the κ_{ij}-axis. The intersection point is $(\kappa_{ij}(n+1), 0)$. If we choose an initial guess $\kappa_{ij}(0) < \kappa_{ij}$ with κ_{ij} being the root of (3), the tangent line to $(\kappa_{ij}(0), F(\kappa_{ij}(0)))$ intersects the κ_{ij}-axis at $(\kappa_{ij}(1), 0)$, where $\kappa_{ij}(0) < \kappa_{ij}(1) < \kappa_{ij}$. This analysis suggests that we choose an initial guess to the left of the root κ_{ij}, i.e., a good initial guess is chosen as $\kappa_{ij}(0) = -\min(\hat{a}_j^2, \hat{b}_j^2) + \rho$ with ρ being a small positive constant. The constant ρ is chosen such that $F(\kappa_{ij}(0)) > 0$.

The algorithm (57) provides a quadratic convergence of $\kappa_{ij}(n)$ to the root of (3), since $\frac{\partial F(\kappa_{ij})}{\partial \kappa_{ij}}$ is nonzero and $\frac{\partial^2 F(\kappa_{ij})}{\partial \kappa_{ij}^2}$ is bounded in the domain of interest, see [39, Th. 1.1] for a proof. Proof of Lemma 2.1 is completed.

APPENDIX B
PROOF OF LEMMA 4.1

We first show that there exists a positive constant k_{ij} such that condition (23) holds. To do so, we partition the interval $(\chi_{ijd}, \chi_{ijR}^M)$ into two intervals $(\chi_{ijd}, \chi_{ij}^*]$ and $(\chi_{ij}^*, \chi_{ijR}^M)$ with χ_{ij}^* being such that

$$\left(\gamma_{ij}' - \frac{\gamma_{ij}}{\chi_{ij}}\right)\Big|_{\forall \chi_{ij} \in (\chi_{ijd}, \chi_{ij}^*]} > 0. \tag{58}$$

From the expressions of γ_{ij} and χ_{ij} in (20), it is trivial to show that there exists $\chi_{ij}^* \in (\chi_{ijd}, \chi_{ijR}^M)$ such that (58) holds.

For all $\chi_{ij} \in (\chi_{ijd}, \chi_{ij}^*]$, we rewrite (24) as

$$\begin{aligned}\varphi_{ij}' = {} & \frac{1 - h(\chi_{ij}, a_{ij}, b_{ij})}{\chi_{ij}}\left(\gamma_{ij}' - \frac{\gamma_{ij}}{\chi_{ij}}\right) \\ & + h'(\chi_{ij}, a_{ij}, b_{ij})\left(k_{ij} - \frac{\gamma_{ij}}{\chi_{ij}}\right).\end{aligned} \tag{59}$$

Since $\frac{1-h(\chi_{ij}, a_{ij}, b_{ij})}{\chi_{ij}} > 0$ and $h'(\chi_{ij}, a_{ij}, b_{ij}) > 0$ for all $\chi_{ij} \in (\chi_{ijd}, \chi_{ij}^*]$, we choose the constant k_{ij} such that

$$k_{ij} \geq \sup\left(\frac{\gamma_{ij}}{\chi_{ij}}\right) \qquad \forall \chi_{ij} \in (\chi_{ijd}, \chi_{ij}^*]. \tag{60}$$

The aforementioned choice of k_{ij} makes condition (23) hold for all $\chi_{ij} \in (\chi_{ijd}, \chi_{ij}^*]$.

For all $\chi_{ij} \in (\chi_{ij}^*, \chi_{ijR}^M)$, we rewrite (24) as

$$\begin{aligned}\varphi_{ij}' = {} & \gamma_{ij}' \frac{1 - h(\chi_{ij}, a_{ij}, b_{ij})}{\chi_{ij}} + h'(\chi_{ij}, a_{ij}, b_{ij}) \\ & \times \left(k_{ij} - \frac{\gamma_{ij}}{\chi_{ij}} - \frac{\gamma_{ij}}{\chi_{ij}^2}\frac{(1 - h(\chi_{ij}, a_{ij}, b_{ij}))}{h'(\chi_{ij}, a_{ij}, b_{ij})}\right).\end{aligned} \tag{61}$$

Since $\gamma_{ij}' \frac{1-h(\chi_{ij}, a_{ij}, b_{ij})}{\chi_{ij}} > 0$ and $h'(\chi_{ij}, a_{ij}, b_{ij}) > 0$ for all $\chi_{ij} \in (\chi_{ij}^*, \chi_{ijR}^M)$, we can choose the constant k_{ij} such that

$$\begin{aligned} & k_{ij} \geq \sup\left(\frac{\gamma_{ij}}{\chi_{ij}} + \frac{\gamma_{ij}}{\chi_{ij}^2}\frac{(1 - h(\chi_{ij}, a_{ij}, b_{ij}))}{h'(\chi_{ij}, a_{ij}, b_{ij})}\right) \\ & \qquad \forall \chi_{ij} \in \chi_{ij} \in (\chi_{ij}^*, \chi_{ijR}^M).\end{aligned} \tag{62}$$

The aforementioned choice of k_{ij} makes condition (23) hold for all $\chi_{ij} \in (\chi_{ij}^*, \chi_{ijR}^M)$. Since a_{ij} and b_{ij} satisfy condition (21), and $\chi_{ij}^* \in (\chi_{ijd}, \chi_{ijR}^M)$, we have $\frac{(1-h(\chi_{ij}, a_{ij}, b_{ij}))}{h'(\chi_{ij}, a_{ij}, b_{ij})}$ is bounded by some constant for all $\chi_{ij} \in (\chi_{ij}^*, \chi_{ijR}^M)$. This implies that the value of k_{ij} that satisfies (62) is finite.

Therefore, the positive constant k_{ij} that satisfies both conditions (60) and (62) makes condition (23) hold for all $\chi_{ij} \in (\chi_{ijd}, \chi_{ijR}^M)$.

To prove Lemma 4.1, we show that the pairwise function φ_{ij} that is defined in (19) satisfies all properties that are listed in (16). Proof of Properties 1–4 is trivial using properties of the p-times differentiable function $h_{ij}(\chi_{ij}, a_{ij}, b_{ij})$ that is listed in (7), and the definition of χ_{ij} in (20). We focus on proving Property 5.

Since the function φ_{ij} is differentiable, Property 5 holds if

$$\begin{aligned} & \varphi_{ij}' < 0 && \forall \chi_{ij} \in (0, \chi_{ijd}) \\ & \varphi_{ij}' = 0 && \text{if } \chi_{ij} = \chi_{ijd} \\ & \varphi_{ij}' > 0 && \forall \chi_{ij} \in (\chi_{ijd}, \chi_{ijR}^M) \\ & \varphi_{ij}' = 0 && \forall \chi_{ij} \in [\chi_{ijR}^M, \infty).\end{aligned} \tag{63}$$

The aforementioned conditions mean that the differentiable function φ_{ij} is decreasing for all $\chi_{ij} \in (0, \chi_{ijd})$, is increasing for all $\chi_{ij} \in (\chi_{ijd}, \chi_{ijR}^M)$, and is constant for all $\chi_{ij} \in [\chi_{ijR}^M, \infty)$.

For all $\chi_{ij} \in (0, \chi_{ijd})$, we have from (24) that

$$\varphi_{ij}' = \frac{\gamma_{ij}'}{\chi_{ij}} - \frac{\gamma_{ij}}{\chi_{ij}^2} \tag{64}$$

where we have used $h(\chi_{ij}, a_{ij}, b_{ij}) = 0$ and $h'(\chi_{ij}, a_{ij}, b_{ij}) = 0$ for all $\chi_{ij} \in (0, \chi_{ijd})$ because a_{ij} and b_{ij} satisfy condition (21). Therefore $\varphi_{ij}' < 0,\ \forall \chi_{ij} \in (0, \chi_{ijd})$ due to $\gamma_{ij}' < 0$, $\forall \chi_{ij} \in (0, \chi_{ijd})$ [see (20)].

For $\chi_{ij} = \chi_{ijd}$, we have $\varphi_{ij}' = 0$ since $\gamma_{ij}\big|_{\chi_{ij}=\chi_{ijd}} = 0$, and $h_{ij}(\chi_{ij}, a_{ij}, b_{ij})\big|_{\chi_{ij}=\chi_{ijd}} = 0$ since $a_{ij} = \chi_{ijd}$ [see (21)].

For all $\chi_{ij} \in (\chi_{ijd}, \chi_{ijR}^M)$, we have already proved that $\varphi_{ij}' > 0$.

For all $\chi_{ij} \in [\chi_{ijR}^M, \infty)$, we have $h(\chi_{ij}, a_{ij}, b_{ij}) = 1$ because a_{ij} and b_{ij} satisfy condition (21). Hence, from (19) we have $\varphi_{ij} = k_{ij}$, which implies that $\varphi_{ij}' = 0$ for all $\chi_{ij} \in [\chi_{ijR}^M, \infty)$. Proof of Lemma 4.1 is completed.

APPENDIX C
PROOF OF THEOREM 4.1

A. Proof of No Collisions and Complete Forwardness of the Closed-Loop System

It is seen from (41) that $\dot{V} \leq 0$. Integrating $\dot{V} \leq 0$ from t_0 to t and using the definition of V in (36) with φ and φ_{ij} given in (25) results in

$$V(t) \leq V(t_0) \tag{65}$$

where

$$\begin{aligned}V(t) = {} & \sum_{i=1}^{N-1}\sum_{j=i+1}^{N}\varphi_{ij}(t) \\ & + \frac{1}{2}\sum_{i=1}^{N}\left(c_1\|\boldsymbol{R}_i(t)(\boldsymbol{p}_i(t) - \boldsymbol{p}_{od}(t))\|^2\right. \\ & \left. + c_2(\phi_i(t) - \phi_{od}(t))^2\right)\end{aligned} \tag{66}$$

and $V(t_0)$ is $V(t)$ with t replaced by t_0, for all $t \geq t_0 \geq 0$. From the condition that is specified in item 4 of Assumption 3.1, and Property 3 of φ_{ij}, we have that the right-hand side of (65) is bounded by a positive constant that depends on the initial conditions. Boundedness of the right-hand side of (65) implies that the left-hand side of (65) must be also bounded. As a result, $\varphi_{ij}(\Delta_{ij}(t))$ must be smaller than some positive constant that depends on the initial conditions for all $t \geq t_0 \geq 0$. From properties of φ_{ij}, see (16), $\Delta_{ij}(t)$, for all $(i,j) \in \mathbb{N}$ and $i \neq j$, must be larger than 1 for all $t \geq t_0 \geq 0$. This, in turn, implies from Lemma 2.1 that there are no collisions between any agents for all $t \geq t_0 \geq 0$. Boundedness of the left-hand side of (65) also implies that of $\boldsymbol{R}_i(\boldsymbol{p}_i(t) - \boldsymbol{p}_{od}(t))$ and $(\phi_i(t) - \phi_{od}(t))$, i.e., $(\boldsymbol{q}_i(t) - \boldsymbol{q}_{od}(t))$ is also bounded for all $t \geq t_0 \geq 0$. Therefore, the closed-loop system (43) is forward complete. Moreover, from (65), we have $\|\boldsymbol{q}_i(t) - \boldsymbol{q}_{od}(t)\| \leq \frac{2}{\min(c_1,c_2)} V(t_0) := A_0$. Hence, we have proved the first two results that are listed in Theorem 4.1.

B. Mismatched Velocity Analysis

We first use Lemma 2.3 to find the equilibrium set, which the trajectories of the closed-loop system (43) converge to. Integration of both sides of (41) yields

$$\int_0^\infty \sum_{i=1}^N \omega_i(t) dt = \varphi(t_0) - \varphi(\infty) \leq \varphi(t_0) \tag{67}$$

where ω_i is given in (42). Indeed, the function $\sum_{i=1}^N \omega_i(t)$ is scalar, nonnegative, and differentiable. Now differentiating $\sum_{i=1}^N \omega_i(t)$ along the solutions of the closed-loop system (43) and using the properties of the function φ_{ij} given in (16) and the function $\psi(\cdot)$ in (40) readily show that $\left|\frac{\mathrm{d}\sum_{i=1}^N \omega_i(t)}{\mathrm{d}t}\right| \leq M \sum_{i=1}^N \omega_i(t)$ with M being a positive constant. Therefore, Lemma 2.3 results in $\lim_{t\to\infty} \sum_{i=1}^N \omega_i(t) = 0$, which implies that $\lim_{t\to\infty} \omega_i(t) = 0$. Hence, from the expression of $\omega_i(t)$ in (42), we have $\lim_{t\to\infty} \big(\Omega_{xi}(t), \Omega_{yi}(t), \Omega_{\phi i}(t)\big) = 0$. Hence, the trajectory $\boldsymbol{q}_i$ of the agent i "almost globally" converges to an (moving with $\boldsymbol{q}_{od}$) equilibrium set $\boldsymbol{\Upsilon}_c$ asymptotically. In the equilibrium set $\boldsymbol{\Upsilon}_c$, we have $\Omega_{xi}(t) = 0$, $\Omega_{yi}(t) = 0$, and $\Omega_{\phi i}(t) = 0$ for all $i \in \mathbb{N}$. The term "almost globally" refers to the fact that the agents start from a set, in which condition (15) holds. Now, the substitution of the limit $\lim_{t\to\infty} \big(\Omega_{xi}(t), \Omega_{yi}(t), \Omega_{\phi i}(t)\big) = 0$ into the time limit of both sides of the closed-loop system (43) to ∞ gives (44).

C. Flock Size

Let $\boldsymbol{q}_{ic} = [x_{ic},\ y_{ic},\ \phi_{ic}]^T$, for all $i \in \mathbb{N}$, be the equilibrium state of the agent i, i.e., $\boldsymbol{q}_{ic} \in \boldsymbol{\Upsilon}_c$, where $\boldsymbol{\Upsilon}_c$ is the equilibrium set as defined previously. In the set $\boldsymbol{\Upsilon}_c$, we have $\Omega_{xi}(t) = 0$, $\Omega_{yi}(t) = 0$, and $\Omega_{\phi i}(t) = 0$ for all $i \in \mathbb{N}$. Hence, from the expression of $\Omega_{xi}(t)$, $\Omega_{yi}(t)$, and $\Omega_{\phi i}(t)$ in (38), we have

$$\begin{aligned}
&\sum_{j=i+1}^N \boldsymbol{\Gamma}_{ijc}^T + \sum_{j=1}^{i-1} \boldsymbol{\Lambda}_{ijc}^T + c_1(\boldsymbol{p}_{ic} - \boldsymbol{p}_{od}(t)) = 0 \\
&\sum_{j=i+1}^N \Xi_{ijc} - \sum_{j=1}^{i-1} \Xi_{jic} + c_2(\phi_{ic} - \phi_{od}(t)) = 0
\end{aligned} \tag{68}$$

where $\boldsymbol{\Gamma}_{ijc}$, $\boldsymbol{\Lambda}_{ijc}$, and Ξ_{ijc} are $\boldsymbol{\Gamma}_{ij}$, $\boldsymbol{\Lambda}_{ij}$, and Ξ_{ij} with $\boldsymbol{q}_i$ replaced by $\boldsymbol{q}_{ic}$ for all $i \in \mathbb{N}$. From (68), we have

$$\begin{aligned}
\left(\sum_{l=i+1}^N \boldsymbol{\Gamma}_{ilc}^T + \sum_{l=1}^{i-1} \boldsymbol{\Lambda}_{ilc}^T\right) - \left(\sum_{k=j+1}^N \boldsymbol{\Gamma}_{jkc}^T + \sum_{k=1}^{j-1} \boldsymbol{\Lambda}_{jkc}^T\right)& \\
+ c_1 \boldsymbol{p}_{ijc} = 0&
\end{aligned} \tag{40}$$

$$\begin{aligned}
\left(\sum_{l=i+1}^N \Xi_{ilc} - \sum_{l=1}^{i-1} \Xi_{lic}\right) - \left(\sum_{k=j+1}^N \Xi_{jkc} - \sum_{k=1}^{j-1} \Xi_{kjc}\right)& \\
+ c_2 \phi_{ijc} = 0&
\end{aligned} \tag{69}$$

where $\boldsymbol{p}_{ijc} = \boldsymbol{p}_{ic} - \boldsymbol{p}_{jc}$ and $\phi_{ijc} = \phi_{ic} - \phi_{jc}$, for all $(i,j) \in \mathbb{N}, j \neq i$. Moreover, all the terms $\boldsymbol{\Gamma}_{ijc}$, $\boldsymbol{\Lambda}_{ijc}$, and Ξ_{ijc} are the vector functions and a function of $\boldsymbol{p}_{ijc}$, $\cos(\phi_{ijc})$, $\sin(\phi_{ijc})$, $\cos(\phi_{ic})$, and $\sin(\phi_{ic})$ only for all $(i,j) \in \mathbb{N}, j \neq j$, see (35) and (2) for the expression of $\boldsymbol{\Gamma}_{ij}$, $\boldsymbol{\Lambda}_{ij}$, and Ξ_{ij} with a note that $\boldsymbol{q}_i$ is replaced by $\boldsymbol{q}_{ic}$ for all $i \in \mathbb{N}$. This observation implies from (69) that $\boldsymbol{p}_{ijc}$ and ϕ_{ijc} must be bounded and depend on $\cos(\phi_{ic})$ and $\sin(\phi_{ic})$ only with $i = 1, \ldots, N$. On the other hand, the flock size $F_L = \sum_{j=i+1}^N \sum_{j=1}^{i-1} \Delta_{ij}$ is a function that depends on $\boldsymbol{p}_{ij}$, $\cos(\phi_{ij})$, $\sin(\phi_{ij})$, $\cos(\phi_i)$, and $\sin(\phi_i)$ only with $(i,j) \in \mathbb{N}, j \neq j$. Therefore, in the equilibrium set $\boldsymbol{\Upsilon}_c$, the flock size, F_{Lc} being F_L with $\boldsymbol{q}_i$ replaced by $\boldsymbol{q}_{ic}$, is a function that depends on $\cos(\phi_{ic})$ and $\sin(\phi_{ic})$ only with $i = 1, \ldots, N$. Moreover, the flock size is bounded whenever its arguments $\boldsymbol{p}_{ij}$, $\cos(\phi_{ij})$, $\sin(\phi_{ij})$, $\cos(\phi_i)$, and $\sin(\phi_i)$ are bounded. Hence, in the equilibrium set $\boldsymbol{\Upsilon}_c$, the flock size is bounded by a function of $\cos(\phi_{ic})$ and $\sin(\phi_{ic})$. Since $\cos(\phi_{ic})$ and $\sin(\phi_{ic})$ are bounded by -1 and 1, there exits a positive constant c_0 such that $F_c \leq c_0$. This completes proof of Theorem 4.1.

References

[1] A. Okubo, "Dynamical aspects of animal grouping: Swarms, schools, flocks and herds," *Adv. Biophys.*, vol. 22, pp. 1–94, 1986.

[2] C. W. Reynolds, "Flocks, herds, and schools: A distributed behavioral model," in *Proc. Comput. Graphics, ACMSIGGRAPH'87 Conf.*, 1987, vol. 21, no. 4, pp. 25–34.

[3] J. Toner and Y. Tu, "Flocks, herds, and schools: A quantitative theory of flocking," *Phys. Rev. E*, vol. 58, no. 4, pp. 4828–4858, 1998.

[4] H. Sridhar, G. Beauchamp and K. Shanker, "Why do birds participate in mixed-species foraging flocks? A large-scale synthesis," *Animal Behav.*, vol. 78, pp. 337–347, 2009.

[5] I. Akyildiz, W. Su, Y. Sankarasubramniam, and E. Cayirci, "A survey on sensor networks," *IEEE Commun. Mag.*, vol. 40, no. 8, pp. 102–114, Aug. 2002.

[6] R. T. Jonathan, R. W. Beard, and B. Young, "A decentralized approach to formation maneuvers," *IEEE Trans. Robot. Autom.*, vol. 19, no. 6, pp. 933–941, Dec. 2003.

[7] D. M. Stipanovica, G. Inalhana, R. Teo, and C. J. Tomlina, "Decentralized overlapping control of a formation of unmanned aerial vehicles," *Automatica*, vol. 40, no. 8, pp. 1285–1296, 2004.

[8] K. D. Do, "Bounded controllers for formation stabilization of mobile agents with limited sensing ranges," *IEEE Trans. Automat. Control*, vol. 52, no. 3, pp. 569–576, Mar. 2007.

[9] D. V. Dimarogonas, S. G. Loizou, K. J. Kyriakopoulos, and M. M. Zavlanos, "A feedback stabilization and collision avoidance scheme for multiple independent non-point agents," *Automatica*, vol. 42, no. 2, pp. 229–243, 2006.

[10] K. D. Do, "Formation tracking control of unicycle-type mobile robots with limited sensing ranges," *IEEE Trans. Control Syst. Technol.*, vol. 16, no. 3, pp. 527–538, May 2008.

[11] N. Leonard and E. Fiorelli, "Virtual leaders,artificial potentials and coordinated control of groups," in *Proc. IEEE Conf. Decision Control*, 2001, pp. 2968–2973.
[12] H. G. Tanner and A. Kumar, "Towards decentralization of multi-robot navigation functions," in *Proc. IEEE Int. Conf. Robot. Autom.*, Barcelona, Spain, 2005, pp. 4132–4137.
[13] S. S. Ge and Y. J. Cui, "New potential functions for mobile robot path planning," *IEEE Trans. Robot. Autom.*, vol. 16, no. 5, pp. 615–620, Oct. 2000.
[14] R. Olfati-Saber and R. M. Murray, "Distributed cooperative control of multiple vehicle formations using structural potential functions," presented at the 15th Int. Fed. Autom. Control World Congr., Barcelona, Spain, 2002.
[15] R. Olfati-Saber, "Flocking for multi-agent dynamic systems: algorithms and theory," *IEEE Trans. Autom. Control*, vol. 51, no. 3, pp. 401–420, Mar. 2006.
[16] W. Ren and R. W. Beard, "Consensus seeking in multi-agent systems under dynamically changing interaction topologies," *IEEE Trans. Autom. Control*, vol. 50, no. 5, pp. 655–661, May 2005.
[17] R. Olfati-Saber and R. Murray, "Flocking with obstacle avoidance: cooperation with limited communication in mobile networks," in *Proc. 42nd IEEE Conf. Decis. Control*, vol. 2, Maui, HI, 2003, pp. 2022–2028.
[18] R. Olfati-Saber and R. Murray, "Consensus problems in networks of agents with switching topology and time-delays," *IEEE Trans. Autom. Control*, vol. 49, no. 9, pp. 1520–1533, Sep. 2004.
[19] Y. Hong, L. Gao, D. Cheng, and J. Hu, "Lyapunov-based approach to multi-agent systems with switching jointly-connected interconnection," *IEEE Trans. Autom. Control*, vol. 52, no. 5, pp. 943–948, May 2007.
[20] D. Gu and Z. Wang, "Leader–follower flocking: Algorithms and experiments," *IEEE Trans. Control Syst. Technol.*, vol. 17, no. 5, pp. 1211–1219, Sep. 2009.
[21] H. Su, X. Wang, and Z. Lin, "Flocking of multi-agents with a virtual leader," *IEEE Trans. Autom. Control*, vol. 54, no. 2, pp. 293–306, Feb. 2009.
[22] V. Gazi and K. M. Passino, "A class of attraction/repulsion functions for stable swarm aggregations," *Int. J. Control*, vol. 77, no. 18, pp. 1567–1579, 2004.
[23] E. Rimon and D. E. Koditschek, "Robot navigation functions on manifolds with boundary," *Adv. Appl. Math.*, vol. 11, no. 4, pp. 412–442, 1990.
[24] V. Gazi and K. Passino, "Stability analysis of social foraging swarms," *IEEE Trans. Syst., Man, Cybern. B: Cybern.*, vol. 34, no. 1, pp. 539–557, Feb. 2004.
[25] A. Das, R. Fierro, V. Kumar, J. Ostrowski, J. Spletzer, and C. Taylor, "A vision based formation control framework," *IEEE Trans. Robot. Autom.*, vol. 18, no. 5, pp. 813–825, Oct. 2002.
[26] J. Cortes, S. Martinez, and T. Karataş, F. Bullo, "Coverage control for mobile sensing networks," *IEEE Trans. Robot. Autom.*, vol. 20, no. 2, pp. 243–255, Apr. 2004.
[27] I. Suzuki and M. Yamashita, "Distributed anonymous mobile robots: Formation of geometric patterns," *SIAM J. Comput.*, vol. 28, no. 4, pp. 1347–1363, 1999.
[28] A. Jadbabaie, J. Lin, and A. S. Morse, "Coordination of groups of mobile autonomous agents using nearest neighbor rules," *IEEE Trans. Autom. Control*, vol. 48, no. 6, pp. 988–1001, Jun. 2003.
[29] J. Cortes, S. Martinez, and F. Bullo, "Spatially-distributed coverage optimization and control with limited-range interactions," *ESAIM. Control, Optim. Calculus Variat.*, vol. 11, pp. 691–719, 2005.
[30] K. D. Do, "Output-feedback formation tracking control of unicycle-type mobile robots with limited sensing ranges," *Robot. Auton. Syst.*, vol. 57, pp. 34–47, 2009.
[31] X. Zheng and P. Palffy-Muhoray, "Distance of closest approach of two arbitrary hard ellipses in two dimensions," *Phys. Rev. E*, vol. 75, pp. 0617091–0617096, 2007.
[32] Y. Choi, W.Wang, Y. Liu, and M. Kim, "Continuous collision detection for two moving elliptic disks," *IEEE Trans. Robot.*, vol. 22, no. 2, pp. 213–224, Apr. 2006.
[33] K. J. Waldron and G. L. Kinzel, *Kinematics Dynamics and Design of Machinery*. New York: Wiley, 2004.
[34] H. Khalil, *Nonlinear Systems*. Englewood Cliffs, NJ: Prentice-Hall, 2002.
[35] M. Krstic, I. Kanellakopoulos, and P. Kokotovic, *Nonlinear and Adaptive Control Design*. New York: Wiley, 1995.
[36] D. Liberzon, *Switching in Systems and Control*. Cambridge, MA: Birkauser, 2003.
[37] K. D. Do and J. Pan, *Control of Ships and Underwater Vehicles: Design for Underactuated and Nonlinear Marine Systems*. New York: Springer-Verlag, 2009.
[38] J. V. Uspensky, *Theory of Equations*. New York: McGraw-Hill, 1948.
[39] C. T. Kelley, *Solving Nonlinear Equations with Newton's Method*. Philadelphia, PA: SIAM, 2003.

Khac Duc Do received the M.E. and Ph.D. degrees (with Distinction) in mechanical engineering from The University of Wollongong, Wollongong, Australia, and The University of Western Australia, Crawley, Australia, in 1999 and 2003, respectively.

He is currently a Research Professor with the School of Mechanical Engineering, The University of Western Australia. His research interests include control of nonlinear systems, control of multiple agents, control of land, air, and ocean vehicles, and control of systems governed by partial differential equations.